



Biominingalization of orange peel peroxidase within metal organic frameworks (OPP–MOFs) for dye degradation

Manish Salgaonkar, Shamraja S. Nadar, Virendra K. Rathod*

Department of Chemical Engineering, Institute of Chemical Technology, Matunga (E), Mumbai, 400019, India

ARTICLE INFO

Keywords:

Biominingalization
Orange peroxidase
Immobilization
Metal organic framework
Dye degradation
Extraction

ABSTRACT

In an attempt to make the biocatalyst preparation economically viable, the peroxidase enzyme extracted from orange peel (*Citrus sinenses*, a fruit waste) was immobilized within metal-organic framework (MOF) via self-assembled biominingalization method. The synthesis of OPP-MOF was accomplished by simply mixing 2-methylimidazole (24 mmol), zinc acetate (8 mmol) and orange peel extract at room temperature within 30 min. The obtained OPP-MOF was confirmed by using different characterization methods such as X-ray diffraction (XRD), Fourier transform infrared (FT-IR) and scanning electron microscopy (SEM). The half-life of OPP-MOF was determined in the temperature range of 40–60 °C which showed 2.1 folds enhanced thermal stability as compared to free enzyme. Further, Michaelis constant (K_M) and maximum rate (V_{max}) values of OPP-MOF were evaluated by Michaelis–Menten kinetics studies which showed higher K_M and lower V_{max} as compared to native peroxidase. Furthermore, peroxidase-MOF retained 48% residual activity after 6th cycle. Also, the storage stability studies of OPP-MOF revealed that there was no significant loss in its activity till 18 days. Finally, immobilized OPP-MOF was used for degradation of methylene blue (MB) and congo red (CR) dye, and it was found to be more efficient and rapid.

1. Introduction

Enzymes are green catalyst which have evolved from an academic curiosity to industrially attractive technology for driving bio-transformation processes. Also, they are widely used for various applications such as biosensors, bioremediation, wastewater treatment, food and pharmaceutical industries [1,2]. Though enzymes have certain inherent advantages, their applicability on industrial level is always a challenge due to difficulties in recovery and reusability for several cycles. The lack of enzyme stability at industrial operational conditions is also an obstacle in their employment in industry [3]. Another problem associated with the use of soluble enzymes (liquid form) is generation of waste in the reaction mixture. Additionally, it contaminates the product (due to presence of enzyme/protein) which ultimately increases the purification cost [4]. These challenges can be addressed by various enzyme immobilization methods which drastically enhance the enzyme properties such as its thermo-stability, tolerance to organic solvents, wide range of pH, selectivity and its employability in industrial/practical uses. The immobilization also eases

the enzyme recovery and re-use, resulting in its cost-effective use focusing its industrial applications [5]. Combined downstream processing includes separation and purification in one step which could be the effective factor to decrease the cost of an enzyme usage on industrial scale. It can be achieved by two ways: (i) by limiting the number of purification steps or simultaneously purifying and (ii) immobilizing the samples. There are some reported strategies for enzyme purification and immobilization in minimum steps, which makes the entire biocatalyst preparation economically viable [6].

In material science, the advanced designs of hybrid material with a specific structure and functionality and its construction/synthesis is a rapidly expanding field. Among different hybrid materials, metal-organic frameworks (MOFs) are a novel class of porous coordination polymers and ultra-porous materials which are composed of inorganic and organic units linked via strong coordination bonds [7–9]. MOFs have developed rapidly and have gained tremendous attention due to their versatile nature, diverse structures, functionalities and their interesting intrinsic properties [10]. Over the past few years, different enzymes such as lipase [11], glucoamylase [12], catalase [13], etc. have

Abbreviations: CR, congo red; DI, deionized water; E_d , deactivation energy; FT-IR, Fourier transform infrared; k_d , deactivation constant; K_M , Michaelis constant; MB, methylene blue; MOF, metal organic framework; OPP, orange peel peroxidase; SDS PAGE, sodium dodecyl sulfate polyacrylamide gel electrophoresis; SEM, scanning electron microscopy; $t_{1/2}$, half-life; TGA, thermogravimetric analysis; V_{max} , maximum rate; XRD, X-ray diffraction; ZIF-8, zeolitic imidazolate framework 8

* Corresponding author.

E-mail address: vk.rathod@ictmumbai.edu.in (V.K. Rathod).

<https://doi.org/10.1016/j.jece.2019.102969>

Received 10 December 2018; Received in revised form 12 February 2019; Accepted 16 February 2019

Available online 16 February 2019

2213-3437/ © 2019 Published by Elsevier Ltd.

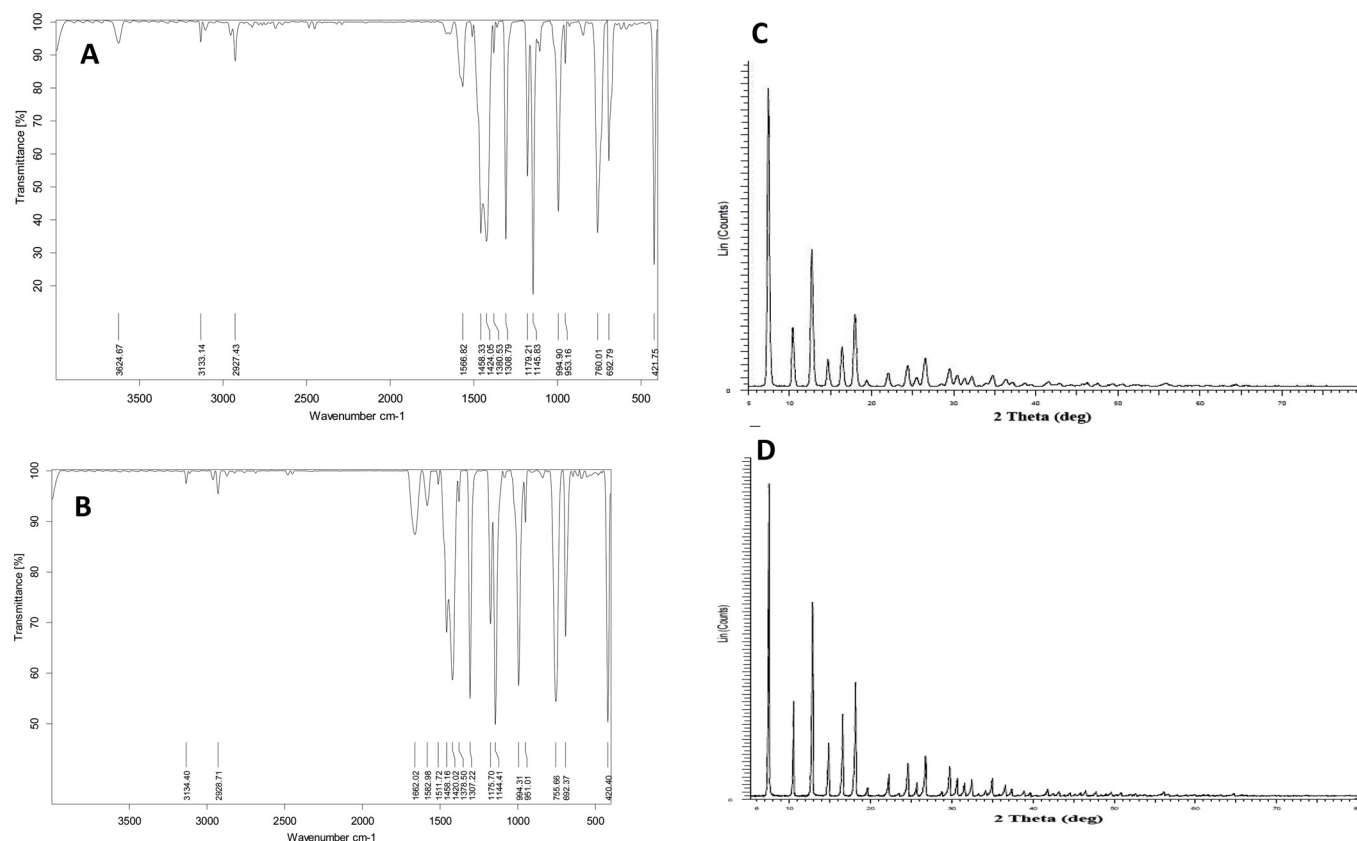


Fig. 1. FT-IR spectra of pure ZIF-8 MOF (without enzyme) (a) and OPP-MOF Powder (b). XRD patterns of pure ZIF-8 MOF (without enzyme) (c) and OPP-MOF (d). SEM images of OPP-MOF (e-f).

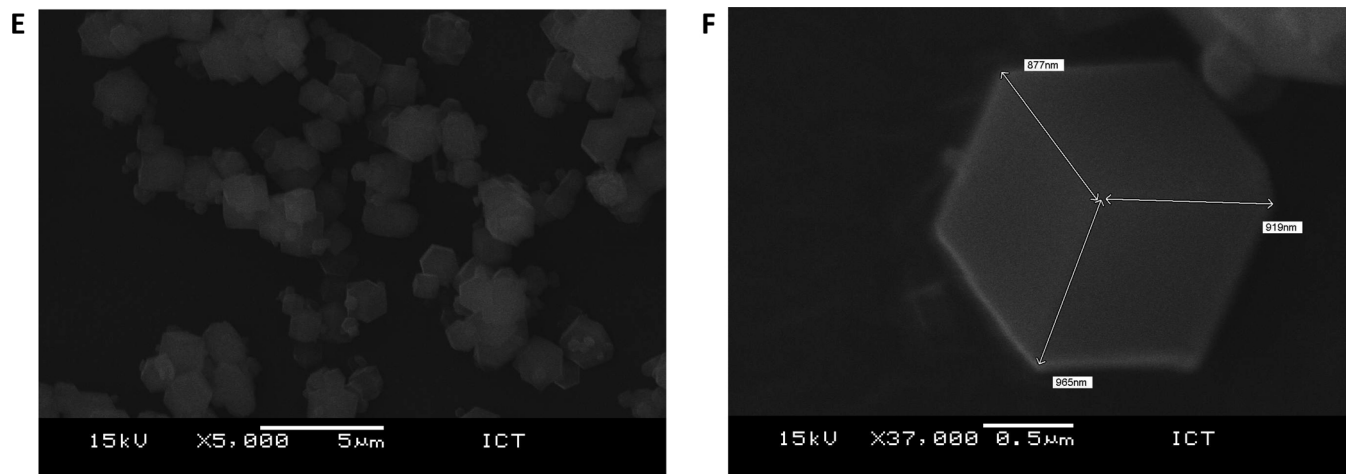


Fig. 1. (continued)

been immobilized onto/within MOF and they have shown outstanding properties such as enhanced thermal stability, storage stability and reusability for multiple cycles. Also, strong interactions of organic part of MOF with proteins prevent the protein molecules from leaching out of the MOF platform during application [13,14]. These futures of MOF make it a potential candidate for immobilizing enzyme for various application.

Enzymes extraction from fruit wastes can be one of the effective ways of utilization of fruit wastes which are obtained in large quantities during the fruit processing. [15] In India, huge fruit wastes are generated annually which is about 5.6 million ton. These wastes are disposed by dumping on the outskirts [16,17]. Utilizing the waste for value added product formation take us one step further in making the process

greener. The peroxidase enzyme from orange peel has been reported to possess wide substrates range, high stability for wide range of pH and temperature. These properties make it an attractive enzyme source for derivation and its valorisation [18]. Earlier, peroxidase immobilization has been reported on various supports such as agarose-chitosan hydrogel [19]. It has been further used for various applications such as environmental remediation (removal of hazardous pollutants, dyes), biomedical, pharmaceutical, nutraceutical, and biotechnological industries [20]. Here, in this work, we have extracted peroxidase from orange peel and immobilized it within MOF, reducing the enzyme purification steps and making it viable for industrial applications. When crude enzyme is mixed with the counterpart of MOFs, enzyme (protein) molecules induce the formation of MOF around enzyme. This results in

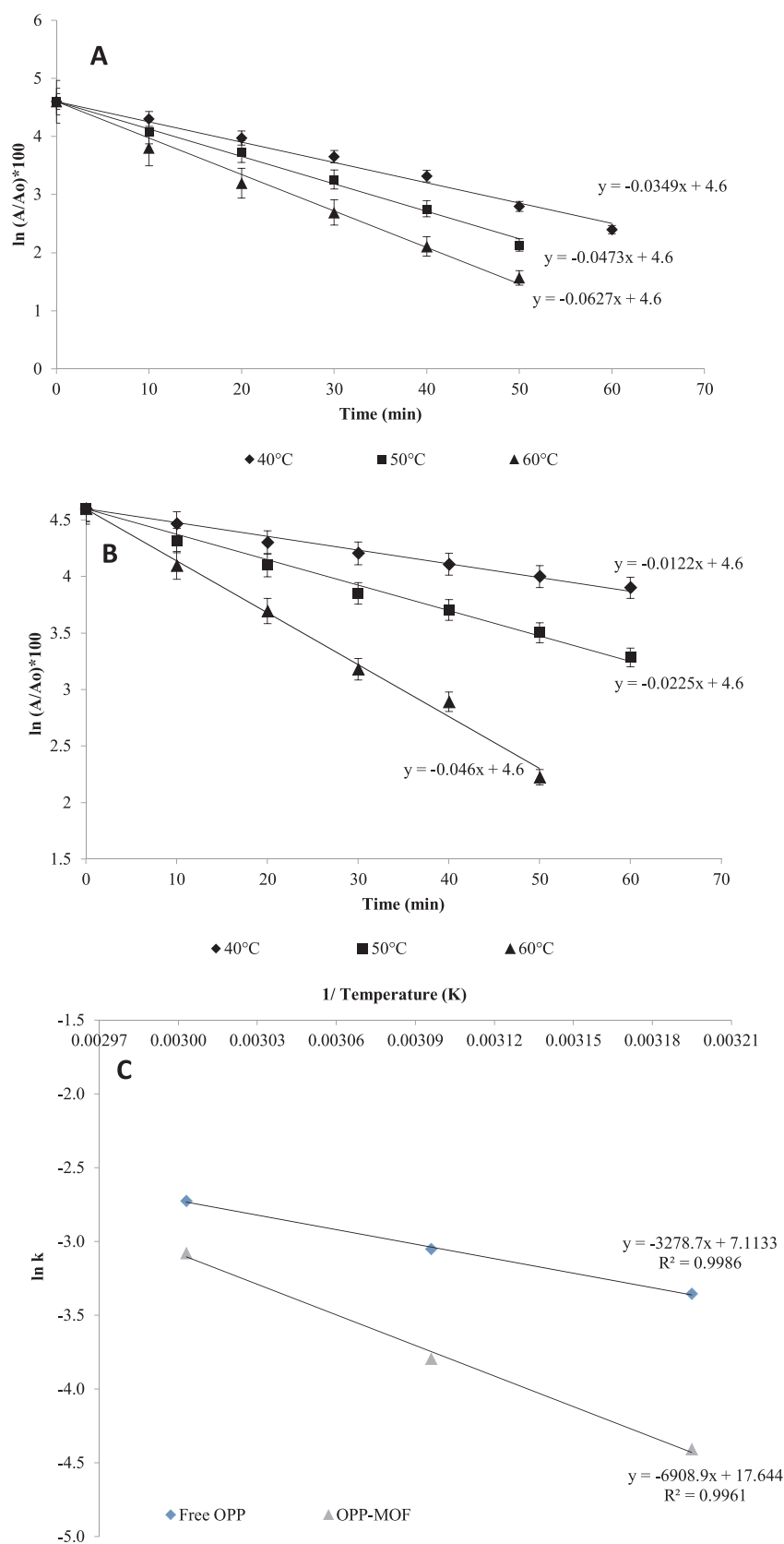


Fig. 2. Thermal inactivation kinetic studies of (a) free OPP (b) and OPP-MOF (c) at 40 °C (◆), 50 °C (■) and 60 °C (▲). Arrhenius plot (d) for inactivation of free OPP and OPP-MOF.

Table 1

Thermal deactivation kinetic parameters: Thermal deactivation constant (K_d), half-life ($t_{1/2}$) and deactivation energy (E_d) of free OPP and OPP-MOF.

Temperature (°C)	K_d (min ⁻¹)			$t_{1/2}$ (min)			E_d (kJ mol ⁻¹)
	40	50	60	40	50	60	
Free OPP	0.0349	0.0473	0.0655	19.9	14.7	10.6	27.25
OPP-MOF	0.0122	0.0225	0.046	56.8	30.8	15.1	57.44

Table 2

Kinetic parameters of free OPP and OPP-MOF.

Form	K_M (μM)	V_{max} (μmol min ⁻¹)
Free OPP	0.3971 ± 0.042	4.7200 ± 0.45
OPP-MOF	0.4159 ± 0.029	4.5721 ± 0.20

Table 3

Dye decolourization of methylene blue and congo red by using free and immobilized OPP.

Form	Dye decolourization (%) ^a	
	Methylene blue	Congo red
OPP-MOF	85.67	89.95
Free OPP	88.33	93.18

^a The dye degradation was carried out for 60 min at room temperature.

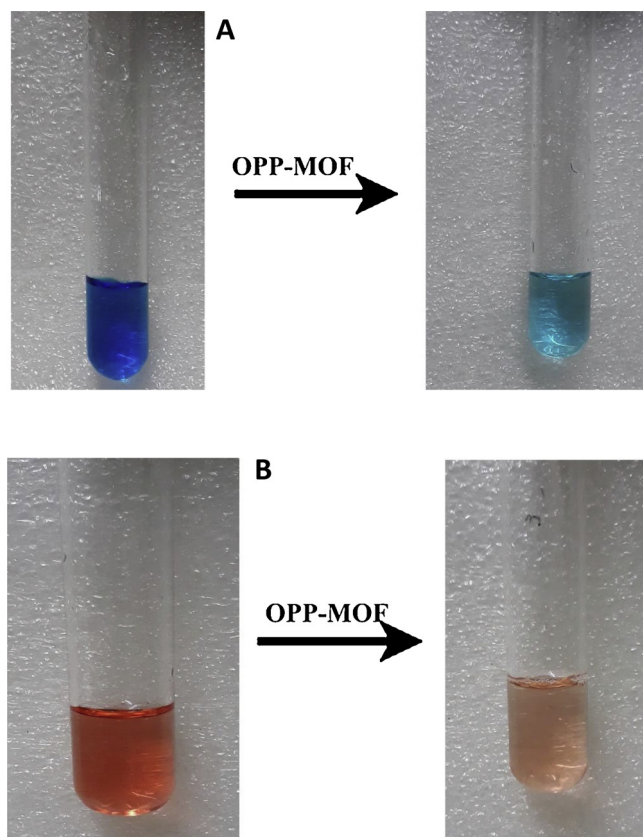


Fig. 3. Photographs of (a) Congo red (CR, 100 ppm) and (b) Methylene blue (MB, 100 ppm) dye degradation with the help of OPP-MOF after 60 min.

one step purification and immobilization of OPP into hybrid MOF, forming OPP-MOF composite. Such peroxidase-encapsulated MOF can be readily prepared via a biomineralization procedure in aqueous solution under mild operational conditions. The characterization of

OPP-MOF was done by XRD and FT-IR to identify crystalline nature and immobilization of OPP within ZIF-8. For the size, shape and morphology analysis, SEM was used. The Michaelis-Menten kinetics parameters were determined for OPP-MOF and the free form of peroxidase. Thermo-kinetic studies were carried out for free enzyme and OPP-MOF to determine the thermal stability in terms of thermal deactivation constant (k_d), half-life ($t_{1/2}$) and deactivation energy (E_d). Finally, different dyes such as methylene blue (MB) and congo red (CR) were degraded by using OPP-MOF.

2. Materials

Fresh unripe oranges (*Citrus sinenses*) were purchased from the local fruit vendors in Matunga (Mumbai, India). Zinc acetate, guaiacol, 2-methylimidazole and hydrogen peroxide were purchased from HiMedia Laboratories Pvt. Ltd, Mumbai, India. All the other reagents were purchased from Sigma Aldrich and used without further purification.

2.1. Preparation of peroxidase extract

Washed orange peels (10 g) were chopped into small pieces (approximately 1 × 1.5 cm) and homogenized into phosphate buffer (0.1 M, pH 7.0) using a blender. The homogenate was filtered through Whatman's filter paper No. 1 and then, filtrate centrifuged (10,000 × g) at 5 °C for 20 min. Further, the supernatant was partially purified by 80% ammonium sulphate. The obtained pellet was re-dissolved and used as the peroxidase source for immobilization.

2.2. Peroxidase activity assay

Peroxidase activity was determined by oxidation of guaiacol in the presence of hydrogen peroxide. Briefly, the guaiacol (2 mL, 10 mM) was added to orange peel extract (100 μL) in the presence of hydrogen peroxide which forms tetraguaiacol (a brownish product, $\epsilon = 26.6 \text{ mM}^{-1} \text{ cm}^{-1}$). The coloured complex was analysed calorimetrically at 470 nm using spectrophotometer (UV-vis spectrophotometer, Japan). One IU of enzyme activity was defined as the amount of enzyme catalysing one μmol of guaiacol in unit time [21].

Protein (enzyme) content was estimated by Bradford protein assay using bovine serum albumin (fraction V) as the standard [22].

2.3. OPP-MOF synthesis

The OPP immobilization within MOF was done by the method reported by Nadar et al. [23]. Briefly, zinc acetate (8 mmol, 14 mL) was mixed with enzyme extract solution (containing protein content of 1.2 mg/mL) of 2-methylimidazole water solution (24 mmol, 14 mL). Then, the mixture was stirred at 200 rpm at 28 ± 2 °C. The white precipitate product (OPP-MOF) was separated by cold centrifugation (8000 × g, 5 °C) for 10 min and washed thrice with DI water.

The synthesis of pure ZIF-8 crystals was done by the above method but without enzyme. This was used for comparison purpose in the subsequent studies.

2.4. Characterization of OPP-MOF

The prepared OPP-MOF was confirmed using Fourier transform infrared (FT-IR, Bruker VERTEX 80-v vacuum FTIR spectrometers, USA) spectroscopy by scanning full spectra ($400\text{--}4000 \text{ cm}^{-1}$). X-ray diffraction (XRD) patterns of pure ZIF-8 and enzyme embedded MOF were recorded by XRD (Philips PW 1830 X-ray Diffraction, Japan) to investigate crystal structures. The morphology of OPP-MOF was analysed using SEM images. For the same, the pitter-coated with conductive thin layer of gold, and images were captured by SEM (JEOL - JSM-6380, Japan) under 10.0 kV. Further, A thermo gravimetric analysis (TGA)

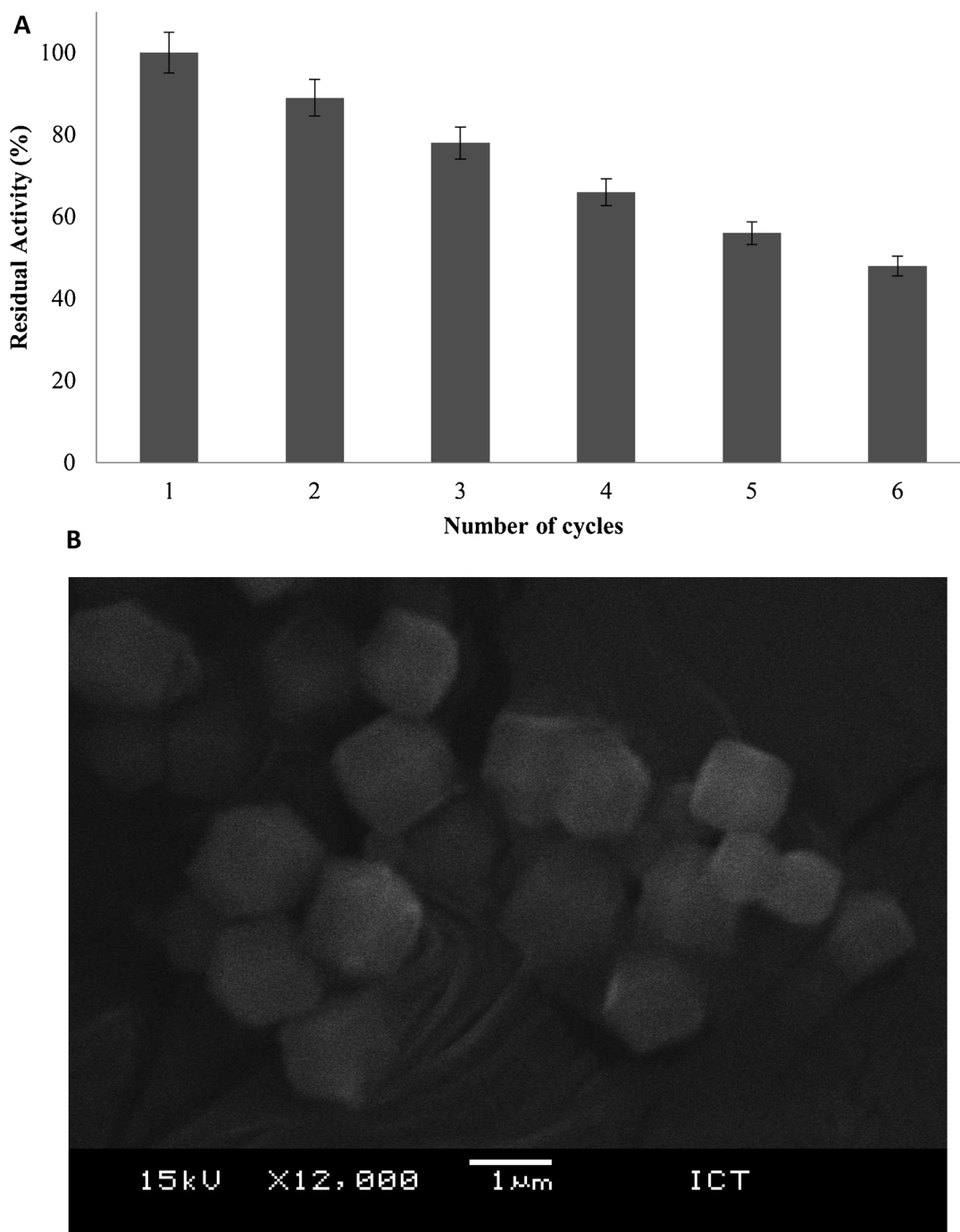


Fig. 4. Reusability studies (a) of OPP-MOF upto 6th cycle and (b) SEM images of OPP-MOF after 6th cycle. The 100% residual activity of peroxidase in first cycle. The experiments were done in triplicate and the error bar represents the percentage error in each set of readings.

STA 449 F3 Jupiter® – NETZSCH instrument was used to calculate the percentage weight loss of OPP-MOF over 25–500 °C in nitrogen atmosphere with a heating rate of 10 °C min⁻¹. Confocal scanning laser microscopy (DMi8 microscope and SP8 scanner Leica, Germany) was used to investigate the presence of fluorescein isothiocyanate (FITC) tagged OPP within the ZIF-8 MOF.

2.5. Properties of OPP-MOF

Thermo-stability was studied in the temperature range of 40–60 °C for enzyme embedded MOFs and thermal deactivation constant (k_d), half-life ($t_{1/2}$) and deactivation energy (E_d) were determined. In Michaelis–Menten kinetics, K_M and V_{max} were evaluated for native OPP

and OPP-MOF. Further, the OPP-MOF was tested for recyclability and was found to be active upto six repetitive cycles. Finally, storage stability of OPP-MOF was evaluated till eighteen days at room temperature and compared with free form. Experimental procedures are given in supplementary information.

2.6. Dye degradation studies

Congo red (100 ppm) and methylene blue (100 ppm) dye solutions were prepared in phosphate buffer. The dye solutions were stirred with free OPP and OPP-MOF which were incubated at room temperature for decolourization till one hour. Control was maintained without addition of enzyme solution. Decolourization was determined by measuring

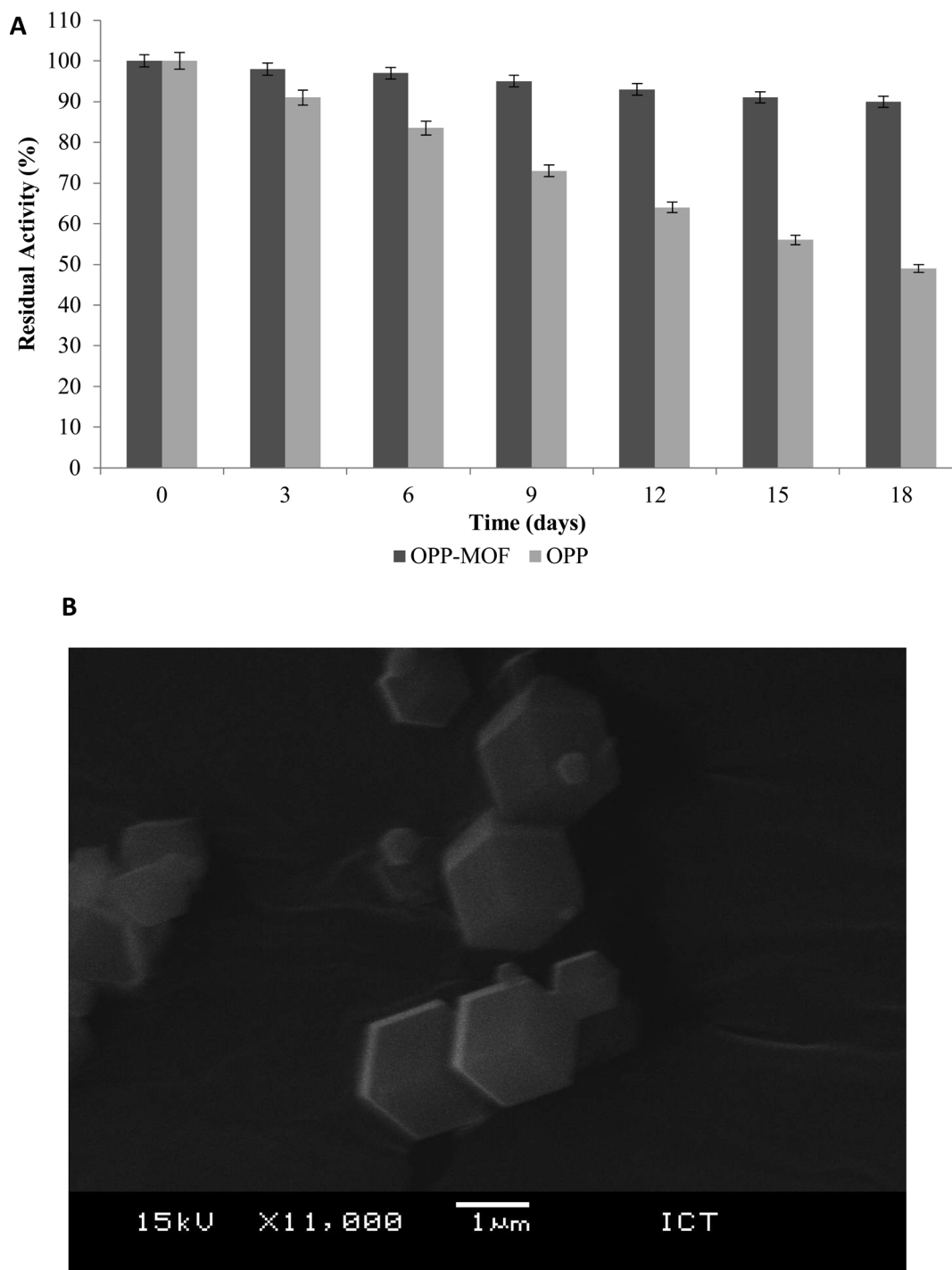


Fig. 5. Storage stability studies till 18 days in phosphate buffer (pH 7.4) (a) and SEM images of OPP-MOF after 18 days of storage (b). The 100% residual activity of peroxidase in first cycle. The experiments were done in triplicate and the error bar represents the percentage error in each set of readings.

absorbance at 495 nm for congo red and 665 nm for methylene blue using spectrophotometric method [24]. The decolourization (%) of dye was determined with respect to buffer.

3. Results and discussion

3.1. Preparation of OPP-MOF

Orange peel was cut into small pieces and stirred with phosphate buffer at 4 °C for 120 min (Fig. S1a). During the extraction procedure, the enzyme stability depends on the pH of extraction buffer. It was

found that OPP showed maximum activity at pH 7.0 (Fig. S2). Post-filtration, the reaction mixture was centrifuged to recover the peroxidase from orange peels. The obtained OPP enzyme solution (after partial purification by 80% saturated ammonium sulphate, Fig. S3) showed activity of 15 U/mL. The SDS PAGE analysis was done for crude and partially purified OPP enzyme with 80 and 100% saturation of ammonium sulphate. Fig. S4 showed few bands after partial purification of OPP with 80% saturation of ammonium sulphate as compared to crude OPP extract. The obtained enzyme solution was further used for immobilization purpose. In a typical immobilization experiment, zinc acetate solution (8 mmol) was added in drop wise manner to the

mixture containing 2-methylimidazole (24 mmol) and enzyme solution (containing activity of 15 U with the total protein content of 1.2 mg/mL). The presence of enzyme (protein) molecules induces the formation of protective framework under physiological conditions, which facilitates crystallization around the biomacromolecules [25,26]. After that, the mixture solution turned cloudy within 30 s and further stirred for 30 min followed by centrifugation and washing with phosphate buffer (pH 7.4, 10 mM) (Fig. S1b). This synthesized MOF successfully entrapped OPP with 99% immobilization yield (determined by Bradford protein assay). The obtained OPP-MOF exhibited activity recovery of 9.2 U/mg (Fig. S1c).

3.2. Characterization of OPP-MOF

The OPP-MOF was characterized and analysed by FT-IR and XRD. The morphology and size were determined by SEM. The amount of immobilized enzyme was determined by TGA.

The immobilization of enzyme was confirmed by comparing OPP-MOF with pure MOF (without enzyme). FT-IR spectra of pure MOF (Fig. 1a) showed the Zn-N stretching band at around 421.75 cm^{-1} . Also, another stretching at 760.01 and 692.79 cm^{-1} is associated with the 2-methylimidazole ring (out-of-plane bending), whereas, the in-plane bending absorption bands were observed at 953.16 and 1308.79 cm^{-1} . Additionally, two peaks at 2927.43 and 3133.14 cm^{-1} , respectively attributed to the aliphatic and aromatic C-H stretching of the 2-methylimidazole which proved the successful synthesis of ZIF-8 [27,28]. Further, in Figs. 1b and S5, the characteristic band present in OPP-MOF was seen at the position 1662.02 cm^{-1} which represents amide I band corresponding to enzyme. It confirmed that enzymes were successfully immobilized within MOF [11,29].

The XRD patterns of the ZIF-8 (without enzyme) and OPP-MOF are shown in Fig. 1c-d. The prominent reflections corresponding to the planes (110), (200), (211), (220), (310), and (222) were observed. The prepared MOF without enzyme exhibited simulated patterns of pure ZIF-8 SOD-type crystal structures (Fig. S6) [30]. After immobilization of OPP, the XRD profile remained similar as that of pure ZIF-8 crystal structure [31]. This consistent and similar diffraction patterns confirm that entrapment of OPP does not change chemical/physical characteristics and properties of original ZIF-8 MOF.

SEM was used to study the morphology and size of prepared OPP-MOF. The OPP-MOF appeared as rhombic dodecahedral shape with dimension of $\sim 875\text{--}975\text{ nm}$ (average size) (Fig. 2e-f). Furthermore, quantitative analysis of entrapped enzyme (protein) within MOF was determined by TGA (Fig. S7). In TGA profile, the decomposition of OPP-MOF was observed in two stages. In first-stage decomposition, a gradual weight loss was seen up to $\sim 23.5\%$ till 200°C which was corresponding to evaporation and removal of H_2O (as a major constituent) and other organic small molecules (guest molecules) from the cavities. In the 2nd decomposition stage ($250\text{--}350^\circ\text{C}$), 9% of weight loss occurred which can be attributed to the decomposition of protein/enzyme molecules within ZIF-8 [13,29]. These all characterization outcomes confirmed the successful encapsulation and immobilization of OPP within ZIF-8 MOF.

3.3. Thermal kinetics and stability studies

High thermo-stability is an additional advantage obtained through immobilization of enzyme within MOF. The enhanced thermal stability would possibly boost the applications of enzyme at industrial scale. The stability of native enzyme and OPP-MOF were determined at different temperatures i.e. 40 , 50 and 60°C till one hour and assayed for activity (calculated as residual activity) with time frame of 10 min. The $t_{1/2}$ and k_d of OPP and OPP-MOF were calculated from Fig. 2a-b and compiled in Table 1. The deactivation constant of immobilized OPP-MOF was found to be much lower than the free peroxidase in the given temperature range. Mostly, at 60°C , free OPP was completely deactivated/

denatured within 50 min of exposure. In contrast, OPP-MOF exhibited an outstanding thermo-stability in terms of half-life within the temperature range of $40\text{--}60^\circ\text{C}$. It exhibited 2.8, 2.1 and 1.4 folds improved half-life as compared to free enzyme at 40 , 50 and 60°C , respectively. This augmentation in thermal stability can be due to the confinement of OPP contributed by MOF which averts the enzyme/protein molecules from aggregating and denaturation [23,32].

Further, E_a for immobilized and free forms of enzyme were calculated from linear fit Arrhenius plot (Fig. 2c). It was seen that 27.3 and 57.4 kJ mol^{-1} energy was required to deactivate native OPP and OPP-MOF respectively. These results indicate that OPP-MOF required much higher energy to change the 3D structure active conformation. This can be attributed to the ZIF-8 framework around enzyme molecules, which primarily functioned as shield to maintain the active structure in high temperature condition. Further, the confocal scanning laser microscopy (CSLM) was carried out for FITC-tagged enzyme molecules to confirm the framework shielding around the OPP (Fig. S8). The CSLM image showed that enzyme molecules were encapsulated within ZIF-8 MOF which confirmed that the structure and functional stability was contributed by frameworks formed during biomineralization processes [33].

3.4. Michaelis-Menten kinetic parameters

Michaelis-Menten parameters (K_M and V_{\max}) of free OPP and OPP-MOF were evaluated by determining initial rates of reaction corresponding to different concentrations of substrate. K_M and V_{\max} values for free and immobilized OPP are mentioned in Table 2. It was observed that value of K_M increased after immobilization of OPP within MOF. This indicated that the enzyme affinity towards substrate slightly decreased which could be probably due to the encapsulation of OPP in the interior of frameworks restricting accessibility [12].

Further, OPP-MOF exhibited lower rate of reaction (V_{\max}) than that of free enzyme mixture. This might be due to the conformational changes while immobilization of enzyme. Also, the mass transfer limitation might lower the rate of reaction for OPP-MOF as compared to free form [34].

3.5. Dye degradation by OPP

The decolourization potential of free OPP and immobilized OPP-MOF was evaluated using two different dyes (MB and CR) by incubating them at room temperature ($28 \pm 2^\circ\text{C}$) (Table 3). The percentage decolourization for methylene blue and congo red dyes was found to be 88.3 and 93.2% using free enzymes. On the other hand, OPP-MOF brought about 85.6 and 89.9% decolourization of methylene blue (Fig. 3a) and congo red (Fig. 3b), respectively. Similar studies have been reported by Pandey and co-workers. They obtained nearly 75% decolourization of various dyes such as congo red, trypan blue and methyl orange with the help of *Azadirachta indica* peroxidase immobilized onto chitosan within 8 h [35]. Also, the reports on manganese peroxidase immobilized within alginate bead showed 78.14% decolourization for Sandal reactive dyes [36].

3.6. Reusability and storage stability studies

While using the enzymes, its reusability holds an essential importance for industrial applications. The recyclability studies of OPP-MOF were performed upto 6th cycle by oxidizing guicol. After six successive cycles, the residual activity was found to be 48% (Fig. 4a). The observed reduction in residual activity during the reusability assay might be due to the enzyme deactivation, damage and handling errors. No free enzyme was found in supernatant even after six consecutive cycles. This suggests that the enzyme (protein content) did not leach out of the MOF platform and the MOF structure was intact. It was verified by SEM image of the OPP-MOF after 6 cycles of use. From Fig. 4b, it

was seen that the structure of OPP-MOF after six cycles remained same as that of fresh OPP-MOF (Fig. 1e–f). This property of OPP-MOF holds the potential to reduce the purification step of protein/enzymes and product at the end of reaction [37,38].

The storage stability of enzyme is another major issue which can be overcome by developing a reliable biocatalyst. In storage stability studies, the OPP-MOF and native peroxidase were incubated at room temperature in aqueous buffer solution. This study was carried out upto 18 days and the enzyme activity was measured after equal interval of three days. The residual activity of the same is shown in Fig. 5a. It was observed that 88% residual activity was retained by OPP-MOF till 18th day of storage. On the other hand, free OPP showed gradual reduction in residual activity, upto 47%, for the same time period. The high storage stability of OPP-MOF was due to the shielding effect of framework around the enzyme molecules which is evident in SEM image (shown in Fig. 5b). Hence, active sites and overall configuration of enzyme molecules did not undergo distortion under storage conditions [39]. The above results highlight the excellent improvement in chemical and conformational stability after framework formation around OPP embedded within MOF.

4. Conclusion

The results obtained in this study demonstrate the successful preparation of MOF induced by peroxidase from orange peels. OPP was successfully extracted and further immobilized via self-assembled biomineralization method. The prepared OPP-MOF showed significant improvement in the thermal stability which was estimated in terms of $t_{1/2}$ and E_a . Further, it exhibited remarkable reusability and storage stability. At the end, rapid degradation of commercial dyes by OPP-MOF exhibited its potential in bioremediation.

Acknowledgements

The authors would like to acknowledge the University Grants Commission (UGC) of India, Government of India for financial assistance in the research work.

Appendix A. Supplementary data

Supplementary material related to this article can be found, in the online version, at doi:<https://doi.org/10.1016/j.jece.2019.102969>.

References

- [1] A. Sepehri, M.H. Sarrafzadeh, Effect of nitrifiers community on fouling mitigation and nitrification efficiency in a membrane bioreactor, *Chem. Eng. Process. Process Intensif.* 128 (2018) 10–18, <https://doi.org/10.1016/j.cep.2018.04.006>.
- [2] J. Chapman, A. Ismail, C. Dinu, Industrial applications of enzymes: recent advances, techniques, and outlooks, *Catalysts* 8 (2018) 238–248, <https://doi.org/10.3390/catal8060238>.
- [3] R.A. Sheldon, S. van Pelt, Enzyme immobilisation in biocatalysis: why, what and how, *Chem. Soc. Rev.* 42 (2013) 6223–6235, <https://doi.org/10.1039/C3CS60075K>.
- [4] R. DiCosimo, J. McAuliffe, A.J. Poulou, G. Bohlmann, Industrial use of immobilized enzymes, *Chem. Soc. Rev.* 42 (2013) 6437–6451, <https://doi.org/10.1039/C3CS35506C>.
- [5] P.V. Iyer, L. Ananthanarayan, Enzyme stability and stabilization-Aqueous and non-aqueous environment, *Process Biochem.* 43 (2008) 1019–1032, <https://doi.org/10.1016/j.procbio.2008.06.004>.
- [6] O. Barbosa, C. Ortiz, Á. Berenguer-Murcia, R. Torres, R.C. Rodrigues, R. Fernandez-Lafuente, Strategies for the one-step immobilization-purification of enzymes as industrial biocatalysts, *Biotechnol. Adv.* 33 (2015) 435–456, <https://doi.org/10.1016/j.biotechadv.2015.03.006>.
- [7] M. Giménez-Marqués, T. Hidalgo, C. Serre, P. Horcajada, Nanostructured metal-organic frameworks and their bio-related applications, *Coord. Chem. Rev.* 307 (2015) 342–360, <https://doi.org/10.1016/j.ccr.2015.08.008>.
- [8] R. Ricco, C. Pfeiffer, K. Sumida, C.J. Sumby, P. Falcaro, S. Furukawa, N.R. Champness, C.J. Doonan, Emerging applications of metal-organic frameworks, *CrystEngComm* 18 (2016) 6532–6542, <https://doi.org/10.1039/C6CE01030J>.
- [9] Y. Cui, B. Li, H. He, W. Zhou, B. Chen, G. Qian, Metal-organic frameworks as platforms for functional materials, *Acc. Chem. Res.* 49 (2016) 483–493, <https://doi.org/10.1021/acs.accounts.5b00530>.
- [10] P. Kumar, K. Vellingiri, K.H. Kim, R.J.C. Brown, M.J. Manos, Modern progress in metal-organic frameworks and their composites for diverse applications, *Microporous Mesoporous Mater.* 253 (2017) 251–265, <https://doi.org/10.1016/j.micromeso.2017.07.003>.
- [11] F. Pitzalis, C. Carucci, M. Naseri, L. Fotouhi, E. Magner, A. Salis, Lipase encapsulation onto ZIF-8: a comparison between biocatalysts obtained at low and high zinc/2-methylimidazole molar ratio in aqueous medium, *ChemCatChem* 10 (2018) 1578–1585, <https://doi.org/10.1002/cctc.201701984>.
- [12] S.S. Nadar, V.K. Rathod, Facile synthesis of glucoamylase embedded metal-organic frameworks (glucoamylase-MOF) with enhanced stability, *Int. J. Biol. Macromol.* 95 (2017) 511–519, <https://doi.org/10.1016/j.ijbiomac.2016.11.084>.
- [13] F.K. Shieh, S.C. Wang, C.I. Yen, C.C. Wu, S. Dutta, L.Y. Chou, J.V. Morabito, P. Hu, M.H. Hsu, K.C.W. Wu, C.K. Tsung, Imparting functionality to biocatalysts via embedding enzymes into nanoporous materials by a de novo approach: size-selective sheltering of catalase in metal-organic framework microcrystals, *J. Am. Chem. Soc.* 137 (2015) 4276–4279, <https://doi.org/10.1021/ja513058h>.
- [14] X. Wu, C. Yang, J. Ge, Green synthesis of enzyme/metal-organic framework composites with high stability in protein denaturing solvents, *Bioprocess. 4* (2017) 24–39, <https://doi.org/10.1186/s40643-017-0154-8>.
- [15] C.S.K. Lin, L.A. Pfaltzgraff, L. Herrero-Davila, E.B. Mubofu, S. Abderrahim, J.H. Clark, A.A. Koutinas, N. Kopsahelis, K. Stamatalatou, F. Dickson, S. Thankappan, Z. Mohamed, R. Brocklesby, R. Luque, Food waste as a valuable resource for the production of chemicals, materials and fuels. Current situation and global perspective, *Energy Environ. Sci.* 6 (2013) 426–443, <https://doi.org/10.1039/c2ee23440h>.
- [16] A. Baiano, Recovery of biomolecules from food wastes - a review, *Molecules* 19 (2014) 14821–14842, <https://doi.org/10.3390/molecules190914821>.
- [17] F. Ruiz-Ruiz, J. Benavides, O. Aguilar, M. Rito-Palomares, Aqueous two-phase affinity partitioning systems: current applications and trends, *J. Chromatogr. A* 1244 (2012) 1–13, <https://doi.org/10.1016/j.chroma.2012.04.077>.
- [18] L.F. Okino-Delgado, C.H. Fleuri, Orange and mango byproducts: agro-industrial waste as source of bioactive compounds and botanical versus commercial description—a review, *Food Rev. Int.* 32 (2015) 1–14, <https://doi.org/10.1080/87559129.2015.1041183>.
- [19] M. Bilal, T. Rasheed, Y. Zhao, H.M.N. Iqbal, J. Cui, “Smart” chemistry and its application in peroxidase immobilization using different support materials, *Int. J. Biol. Macromol.* 119 (2018) 278–290, <https://doi.org/10.1016/j.ijbiomac.2018.07.134>.
- [20] C. Barrios-Estrada, M. de J. Rostro-Alanis, A.L. Parra, M.P. Belleville, J. Sanchez-Marciano, H.M.N. Iqbal, R. Parra-Saldivar, Potentialities of active membranes with immobilized laccase for Bisphenol A degradation, *Int. J. Biol. Macromol.* 108 (2018) 837–844, <https://doi.org/10.1016/j.ijbiomac.2017.10.177>.
- [21] M.C. Lakshmi, K.S.M.S. Raghavarao, Downstream processing of soy hull peroxidase employing reverse micellar extraction, *Biotechnol. Bioprocess Eng.* 15 (2010) 937–945, <https://doi.org/10.1007/s12257-010-0071-6>.
- [22] M.M. Bradford, A rapid and sensitive method for the quantitation of microgram quantities of protein utilizing the principle of protein-dye binding, *Anal. Biochem.* 72 (1976) 248–254, [https://doi.org/10.1016/0003-2697\(76\)90527-3](https://doi.org/10.1016/0003-2697(76)90527-3).
- [23] S.S. Nadar, V.K. Rathod, Encapsulation of lipase within metal-organic framework (MOF) with enhanced activity intensified under ultrasound, *Enzyme Microb. Technol.* 108 (2018) 11–20, <https://doi.org/10.1016/j.enzmictec.2017.08.008>.
- [24] S.B. Jadhav, R.S. Singhal, Polysaccharide conjugated laccase for the dye decolorization and reusability of effluent in textile industry, *Int. Biodeterior. Biodegrad.* 85 (2013) 271–277, <https://doi.org/10.1016/j.ibiod.2013.08.009>.
- [25] Y. Yin, C. Gao, Q. Xiao, G. Lin, Z. Lin, Z. Cai, H. Yang, Protein-metal organic framework hybrid composites with intrinsic peroxidase-like activity as a colorimetric biosensing platform, *ACS Appl. Mater. Interfaces* 8 (2016) 29052–29061, <https://doi.org/10.1021/acsami.6b09893>.
- [26] K. Liang, R. Ricco, C.M. Doherty, M.J. Styles, S. Bell, N. Kirby, S. Mudie, D. Haylock, A.J. Hill, C.J. Doonan, P. Falcaro, Biomimetic mineralization of metal-organic frameworks as protective coatings for biomacromolecules, *Nat. Commun.* 6 (2015) 7240, <https://doi.org/10.1038/ncomms8240>.
- [27] M. Jian, B. Liu, R. Liu, J. Qu, H. Wang, X. Zhang, Water-based synthesis of zeolitic imidazolate framework-8 with high morphology level at room temperature, *RSC Adv.* 5 (2015) 48433–48441, <https://doi.org/10.1039/C5RA04033G>.
- [28] K. Kida, M. Okita, K. Fujita, S. Tanaka, Y. Miyake, Formation of high crystalline ZIF-8 in an aqueous solution, *CrystEngComm* 15 (2013) 1794–1806, <https://doi.org/10.1039/c2ce26847g>.
- [29] F. Lyu, Y. Zhang, R.N. Zare, J. Ge, Z. Liu, One-pot synthesis of protein-embedded metal-organic frameworks with enhanced biological activities—supporting information, *Nano Lett.* 14 (2014) 5761–5765, <https://doi.org/10.1021/nl5026419>.
- [30] H. He, H. Han, H. Shi, Y. Tian, F. Sun, Y. Song, Q. Li, G. Zhu, Construction of thermophilic lipase-embedded metal-organic frameworks via biomimetic mineralization: a biocatalyst for ester hydrolysis and kinetic resolution, *ACS Appl. Mater. Interfaces* 8 (2016) 24517–24524, <https://doi.org/10.1021/acsami.6b05538>.
- [31] X. Wu, J. Ge, C. Yang, M. Hou, Z. Liu, Facile synthesis of multiple enzyme-containing metal-organic frameworks in a biomolecule-friendly environment, *Chem. Commun.* 51 (2015) 13408–13411, <https://doi.org/10.1039/C5CC05136C>.
- [32] F.S. Liao, W.S. Lo, Y.S. Hsu, C.C. Wu, S.C. Wang, F.K. Shieh, J.V. Morabito, L.Y. Chou, K.C.W. Wu, C.K. Tsung, Shielding against unfolding by embedding enzymes in metal-organic frameworks via a de novo approach, *J. Am. Chem. Soc.* 139 (2017) 6530–6533, <https://doi.org/10.1021/jacs.7b01794>.
- [33] M. Salgaonkar, S.S. Nadar, V.K. Rathod, Combi-metal organic framework (Combi-MOF) of α -amylase and glucoamylase for one pot starch hydrolysis, *Int. J. Biol. Macromol.* 113 (2018) 464–475, <https://doi.org/10.1016/j.ijbiomac.2018.02.092>.
- [34] J. Cui, Y. Feng, T. Lin, Z. Tan, C. Zhong, S. Jia, Mesoporous metal-organic

- framework with well-defined cruciate flower-like morphology for enzyme immobilization, *ACS Appl. Mater. Interfaces* (2017) (2017) 10587–10594, <https://doi.org/10.1021/acsami.7b00512>.
- [35] V.P. Pandey, J. Rani, N. Jaiswal, S. Singh, M. Awasthi, A.K. Shasany, S. Tiwari, U.N. Dwivedi, Chitosan immobilized novel peroxidase from *Azadirachta indica*: characterization and application, *Int. J. Biol. Macromol.* 104 (2017) 1713–1720, <https://doi.org/10.1016/j.ijbiomac.2017.02.047>.
- [36] M. Bilal, M. Asgher, Sandal reactive dyes decolorization and cytotoxicity reduction using manganese peroxidase immobilized onto polyvinyl alcohol-alginate beads, *Chem. Cent. J.* 9 (2015) 1–14, <https://doi.org/10.1186/s13065-015-0125-0>.
- [37] Y. Chen, S. Han, X. Li, Z. Zhang, S. Ma, Why does enzyme not leach from metal-organic frameworks (MOFs)? Unveiling the interactions between an enzyme molecule and a MOF, *Inorg. Chem.* 53 (2014) 10006–10008, <https://doi.org/10.1021/ic501062r>.
- [38] X. Wu, C. Yang, J. Ge, Z. Liu, Polydopamine tethered enzyme/metal–organic framework composites with high stability and reusability, *Nanoscale*. 7 (2015) 18883–18886, <https://doi.org/10.1039/C5NR05190H>.
- [39] K. Liang, C.J. Coghlan, S.G. Bell, C. Doonan, P. Falcaro, Enzyme encapsulation in zeolitic imidazolate frameworks: a comparison between controlled co-precipitation and biomimetic mineralisation, *Chem. Commun.* 52 (2015) 473–476, <https://doi.org/10.1039/c5cc07577g>.